Neuron, Vol. 32, 1027–1040, December 20, 2001, Copyright ©2001 by Cell Press

Kinase-Independent Requirement of EphB2 Receptors in Hippocampal Synaptic Plasticity

Ilona C. Grunwald,[1,6] Martin Korte,[2,6] David Wolfer,[3] George A. Wilkinson,[1] Klaus Unsicker,[4] Hans-Peter Lipp,[3] Tobias Bonhoeffer,[2] and Rüdiger Klein[1,5]

[1]Department of Molecular Neurobiology
[2]Department of Cellular and Systems Neurobiology
Max-Planck-Institute of Neurobiology
Am Klopferspitz 18a
D-82152 Martinsried
Germany
[3]Institute of Anatomy and Centre for Neuroscience
University of Zürich
CH-8057 Zürich
Switzerland
[4]Department of Anatomy and Cell Biology III
University of Heidelberg
D-69120 Heidelberg
Germany

Summary

During development, Eph receptors mediate the repulsive axon guidance function of ephrins, a family of membrane attached ligands with their own receptor-like signaling potential. In cultured glutamatergic neurons, EphB2 receptors were recently shown to associate with NMDA receptors at synaptic sites and were suggested to play a role in synaptogenesis. Here we show that Eph receptor stimulation in cultured neurons modulates signaling pathways implicated in synaptic plasticity, suggesting cross-talk with NMDA receptor-activated pathways. Mice lacking EphB2 have normal hippocampal synapse morphology, but display defects in synaptic plasticity. In *EphB2*$^{-/-}$ hippocampal slices, protein synthesis-dependent long-term potentiation (LTP) was impaired, and two forms of synaptic depression were completely extinguished. Interestingly, targeted expression of a carboxy-terminally truncated form of EphB2 rescued the *EphB2* null phenotype, indicating that EphB2 kinase signaling is not required for these EphB2-mediated functions.

Introduction

Activity-dependent synaptic plasticity and memory formation require N-methyl-D-aspartate (NMDA)-type glutamate receptors expressed on the postsynaptic side of excitatory synapses (Bliss and Collingridge, 1993). Ca^{2+} permeation of the NMDA receptor is crucial during synapse formation and for the regulation of synaptic strength in the adult (Bliss and Collingridge, 1993). Strong activation of NMDA receptors by high-frequency stimulation produces an increase in synaptic efficacy, known as long-term potentiation (LTP). Late phases of LTP (L-LTP, >120 min), but not early phases of LTP (E-LTP) require protein synthesis (reviewed in Impey et al., 1999). In contrast, low-frequency stimulation produces a reduction in synaptic efficacy in the CA1 region of the hippocampus, so-called long-term depression (LTD) (Dudek and Bear, 1993). While LTP is hypothesized to be a cellular correlate for long-term memory, LTD may be a process to refine synaptic connections (Katz and Shatz, 1996). In the adult hippocampus, low-frequency stimulation at synapses that have recently undergone LTP can depress synaptic efficacy, a phenomenon known as depotentiation (O'Dell and Kandel, 1994). LTD and depotentiation share many features, including a requirement for NMDA receptors (reviewed in Wagner and Alger, 1996).

The molecular mechanisms underlying excitatory synaptic transmission in the hippocampus and other brain structures involved in learning and memory are not well understood. NMDA receptors form multicomponent complexes and interact with dozens (perhaps hundreds) of postsynaptic proteins, as recently identified by mass spectrometry techniques (Husi et al., 2000). Components of the NMDA receptor complex include cytoskeletal and scaffold proteins, signaling enzymes such as serine/threonine and tyrosine kinases, and their phosphatase counterparts, as well as other types of receptors (reviewed in Garner et al., 2000; Soderling and Derkach, 2000). Although some of the components are required for NMDA receptor-mediated synaptic plasticity (reviewed in Soderling and Derkach, 2000), for the vast majority of components, their role in NMDA receptor-mediated functions remains to be established.

Using biochemical techniques, EphB2, a member of the B subclass of Eph receptor tyrosine kinases, was recently shown to interact with NMDA receptors at excitatory synapses (Dalva et al., 2000; reviewed in Drescher, 2000). Based on earlier observations that showed EphB receptors and their ephrinB ligands localized at synaptic sites in cultured hippocampal neurons (Torres et al., 1998), it was demonstrated that EphB2 efficiently coimmunoprecipitated the obligatory subunit NR1 of the NMDA receptor (Dalva et al., 2000). Short-term (60 min) treatment of cultured cortical neurons with a soluble, active form of ephrinB1 (ephrinB1-Fc) induced the formation of EphB2/NR1 coclusters in an EphB2 kinase-independent fashion. Long-term (4 days) treatment with ephrinB1-Fc increased the number of synaptic release sites 2-fold. This presynaptic event was shown to be EphB2 kinase dependent (reviewed in Klein, 2001; Drescher, 2000).

The role of EphB2 in NMDA receptor-mediated functions in the adult brain remains unclear. Until recently, Eph receptors have been studied exclusively in early developmental processes, including compartment boundary formation, cell migration, and axon guidance (reviewed in Flanagan and Vanderhaeghen, 1998; Wilkinson, 2000). In the mouse, EphB2 receptors are required for the formation of forebrain commissures (Henkemeyer et al., 1996), for retinal axon path finding (Birgbauer et al., 2000), for normal vestibular function (Cowan et al., 2000), and for the development of the vasculature (Adams et

[5]Correspondence: rklein@neuro.mpg.de
[6]These authors contributed equally to this work.

al., 1999). Curiously, most EphB2 functions during development do not require an active EphB2 kinase domain. A hypomorphic allele of *EphB2*, which encoded a non-catalytic truncated form of EphB2 fused to β-galactosidase (EphB2-β-gal), rescued EphB2-mediated functions, at least in certain genetic backgrounds (Birgbauer et al., 2000; Henkemeyer et al., 1996). Soluble EphB2-Fc was able to interact with axonal ephrinB ligands (Henkemeyer et al., 1996), which themselves can have receptor-like properties (reviewed in Brückner and Klein, 1998). These and other data suggested important roles for ephrinB reverse signaling (reviewed in Wilkinson, 2000).

Evidence for Eph receptor functions in the adult brain is rather scarce. Using immunogold electron microscopy, EphB2 and EphB3 receptors were found to be localized on the postsynaptic side of CA1 region synapses in the adult hippocampus (Buchert et al., 1999). EphA and ephrinA subclass molecules were implicated in hippocampal LTP by perfusion of slices in Fc fusion proteins (Gao et al., 1998). Similarly, intrahippocampal infusion of EphA5-Fc and ephrinA5-Fc changed the performance of mice in learning tasks (Gerlai et al., 1999). However, since Fc fusion proteins both activate their respective binding partners and interfere with endogenous ephrin-Eph interactions, the molecular mechanisms underlying the observed defects remained unclear. Here we provide genetic evidence for EphB2 being an essential component of hippocampal synaptic plasticity. Lack of EphB2 in germline targeted mice caused strong defects in LTD and depotentiation and modest deficiencies in L-LTP. Targeted expression of a catalytically inactive EphB2 receptor rescued the EphB2-dependent depotentiation and L-LTP defects as well as the behavioral impairments, indicating that EphB2 kinase signaling is dispensable for its functions at excitatory synapses.

Results

Expression Patterns of Eph Receptors and EphrinB Ligands in the Adult Hippocampus

We performed in situ hybridization experiments to analyze which Eph receptors and ephrinB ligands were expressed in adult hippocampi. Three EphB receptors (EphB1 through EphB3) and EphA4, which also binds ephrinB ligands, were found to be expressed in overlapping and specific patterns. While EphB2 and EphA4 were expressed in all regions of the hippocampal formation (Figures 1C and 1G), EphB1 mRNA was absent in CA1, highly enriched in the CA3 region and expressed at low levels in the dentate gyrus (Figure 1A). The EphB3 expression pattern was complementary to EphB1, i.e., high levels in CA1, barely detectable in CA3 and absent in dentate gyrus (Figure 1E). EphB4 was not included in this analysis, since its expression is restricted to non-neuronal tissues (Shin et al., 2001). Regarding ephrinB ligands, ephrinB1 expression was barely detectable in the CA regions, while ephrinB2 expression was mostly confined to CA1, absent in CA3, and weak in the dentate gyrus, resembling somewhat EphB3 expression (Figures 1B, 1D, and 1E). The ephrinB3 expression pattern was rather unique with substantial levels in CA1, low levels in CA3, and prominent levels in the dentate gyrus (Figure 1F). Since all three EphB receptors are known to interact with all three ephrinB ligands (Flanagan and Vanderhaeghen, 1998), these expression patterns suggest multiple sites of interactions throughout the hippocampal circuits. As described below, we have concentrated our

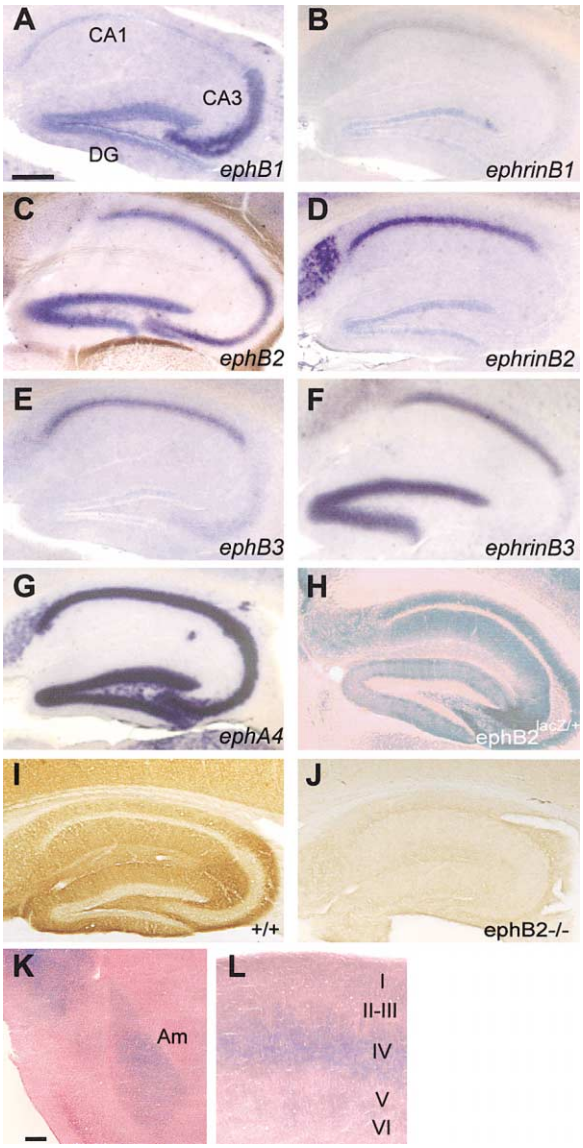

Figure 1. Eph Receptors and EphrinB Ligands Are Expressed in Overlapping and Distinct Patterns in the Adult Hippocampus

(A–G) In situ hybridization analyses of hippocampal sections of adult wild-type mice using the indicated digoxigenin-labeled antisense probes. Staining patterns ranged from regionally restricted ([A], *EphB1* in CA3 region) to general ([C], *EphB2* in CA1, CA3, DG), and from weak ([B], ephrinB1 in CA1 and CA3) to very strong ([G], ephA4).

(H) β-galactosidase staining pattern of mice heterozygous for the *EphB2*^{lacZ} allele. Note strong expression of EphB2-β-gal protein on neurites.

(I and J) EphB2 immunoreactivity matching the pattern of EphB2-β-gal in wild-type (I), but not *EphB2*$^{-/-}$ mice (J).

(K and L) β-galactosidase staining on coronal *EphB2*$^{lacZ/+}$ mice. EphB2-β-gal is detected in the basolateral amygdala (K) and in the neocortex, especially layer IV (L).

Abbreviations: DG (dentate gyrus). Scale bars: (A–J), 1 mm; (K and L), 100 μm.

efforts on EphB2 and therefore performed additional experiments to localize EphB2 protein. Immunohistochemistry using an EphB2-specific antiserum revealed immunoreactivity on neurites of CA1, CA3, and dentate gyrus, whereas pyramidal cell soma appeared largely unstained (Figures 1I and 1J). Similar results were obtained using the *EphB2^{lacZ}* knockin mice (Figure 1H). Additional sites of EphB2 expression included amygdala, neocortex (Figures 1K and 1L), and cerebellar granule cells (data not shown).

Interaction of EphB2 and EphB2-β-gal with NR1

EphB2, but not EphA4, was recently shown to interact with the NR1 subunit of NMDA-type glutamate receptors in cultured neurons (Dalva et al., 2000). To perform coimmunoprecipitation experiments from brain lysates, we generated an EphB2-specific antiserum against the poorly conserved cytoplasmic SAM domain (see supplemental data at http://www.neuron.org/cgi/content/full/32/6/1027/DC1). Highest levels of EphB2 protein were detected in neocortex and cerebellum of wild-type and *EphB3$^{-/-}$* mice, whereas *EphB2$^{-/-}$* mice did not contain immunoreactive material (Figure 2A). EphB2 protein could be coimmunoprecipitated with NR1 from wild-type adult hippocampus, cerebellum, and neocortex, but not from *EphB2$^{-/-}$* tissue (Figure 2B). Conversely, immunoprecipitation of EphB2 from neocortex coimmunoprecipitated NR1 protein very efficiently (Figure 2B). Because in heterologous cells the interaction of EphB2 and NR1 required only the extracellular domains of both proteins (Dalva et al., 2000), we investigated the interaction of C-terminally truncated EphB2 with NR1 in tissue lysates of *EphB2^{lacZ}* mutants. Using different brain tissues of adult *EphB2$^{lacZ/lacZ}$* mice, we visualized the EphB2-β-gal fusion protein as a 190 kDa species, which was not detectable in wild-type tissue (Figure 2C). NR1 was coimmunoprecipitated with EphB2-β-gal in a kinase domain-independent manner (Figure 2D). No EphB2-β-gal was coimmunoprecipitated with NR1 when anti-β-gal antibodies were used with wild-type tissue lysates (Figure 2D). We also used anti-phospho-EphB2 antibodies to immunoprecipitate EphB2 (Dalva et al., 2000). These antibodies recognize a conserved double tyrosine motif in the juxtamembrane region of EphBs that serves as a docking site for cytoplasmic effector proteins (reviewed in Wilkinson, 2000). Because this sequence motif is retained in the EphB2-β-gal fusion protein (Henkemeyer et al., 1996), we asked whether these tyrosine residues were phosphorylated. IP using anti-phospho-EphB2 yielded modest levels of a 120 kDa protein in an anti-EphB2 immunoblot specifically from wild-type, but not from *EphB2$^{-/-}$* tissue (Figure 2E). Curiously, anti-phospho-EphB2 antibodies, but not antibodies directed against the EphB2-SAM domain, also detected EphB2-β-gal in tissue derived from *EphB2$^{lacZ/lacZ}$* mice (Figure 2E). In summary, we conclude that in *EphB2$^{lacZ/lacZ}$* mutants, the interaction with NR1 is rescued. Moreover, the EphB2-β-gal fusion protein, although devoid of a kinase domain, may retain some of its signaling properties by presenting phospho-tyrosine residues to cytoplasmic effector molecules.

EphB Receptor Stimulation Activates and Counteracts Signaling Pathways Implicated in Synaptic Plasticity

The consequences of EphB/NR1 complexes for signaling events on the postsynaptic side are poorly understood. We asked whether in neurons EphB signaling would regulate pathways known to be important for synaptic plasticity and whether other potent stimuli, such as glutamate or brain-derived neurotrophic factor (BDNF), would affect EphB2 receptor activation and signaling. Stimulation of cultured mature hippocampal and cortical neurons (7DIV [Kavalali et al., 1999]) with clustered ephrinB1-Fc caused rapid autophosphorylation of EphB2, whereas no autophosphorylation was observed in cells stimulated with either BDNF or glutamate (Figure 3A). Costimulation with ephrinB1-Fc and glutamate did not lead to significant changes (perhaps a slight reduction at 5 min) in the levels of autophosphorylated EphB2, indicating that NMDA receptor activation did not interfere with ephrinB1-EphB2 interactions and EphB2 dimerization.

The ERK/MAPK pathway has previously been shown to play important functions during synaptic plasticity processes, such as LTP (reviewed in Impey et al., 1999). Stimulation of cultured hippocampal neurons with clustered ephrinB1-Fc led to a subtle yet significant increase in phosphorylation of p42ERK with somewhat delayed kinetics (20 min), compared to the rapid (5 min) kinetics observed with glutamate (Figure 3B). Interestingly, glutamate-induced phosphorylation of p42ERK was reduced to almost baseline levels by preincubation with clustered ephrinB1-Fc (Figures 3B and 3C). This effect was seen only after 60 min and correlated with the time required for coclustering of EphB2 and NR1 (Dalva et al., 2000). We next investigated the effect of A-type Eph receptors, which appear not to associate with NMDA receptors (Dalva et al., 2000). Clustered ephrinA1-Fc reduced the phosphorylation of p42ERK to a lesser extend, supporting the notion that direct interaction between EphB and NMDA receptors facilitates this process (Figure 3C, left panel). The fact that in *EphB2$^{-/-}$* neurons ephrinB1-Fc is still effective in pMAPK suppression indicates that other EphB receptors can compensate for the absence of EphB2 (Figure 3C, right panel). This cross-talk is likely to be specific for Eph and NMDA receptors, since BDNF-induced MAPK phosphorylation was not counteracted by ephrins (Figure 3C).

The cyclic adenosine monophosphate-responsive, element binding protein (CREB) becomes rapidly phosphorylated on Ser133 in response to a variety of intracellular pathways including the ERK/MAPK pathway (Impey et al., 1998). Phospho-CREB was detected by immunoblotting after 20 min of ephrinB1 stimulation, correlating with the kinetics of phospho-ERK. However, phosphorylation of CREB was sustained for 60 min and glutamate-induced CREB phosphorylation was neither blocked nor enhanced by clustered ephrinB1, suggesting that EphB2 and NR1 independently regulated CREB phosphorylation through pathway(s) separate from ERKs.

Src family kinases, including Src and Fyn, are downstream targets of Eph receptors at least in transfected cell systems (for review, see Brückner and Klein, 1998), are part of the NMDA receptor complex (Husi et al.,

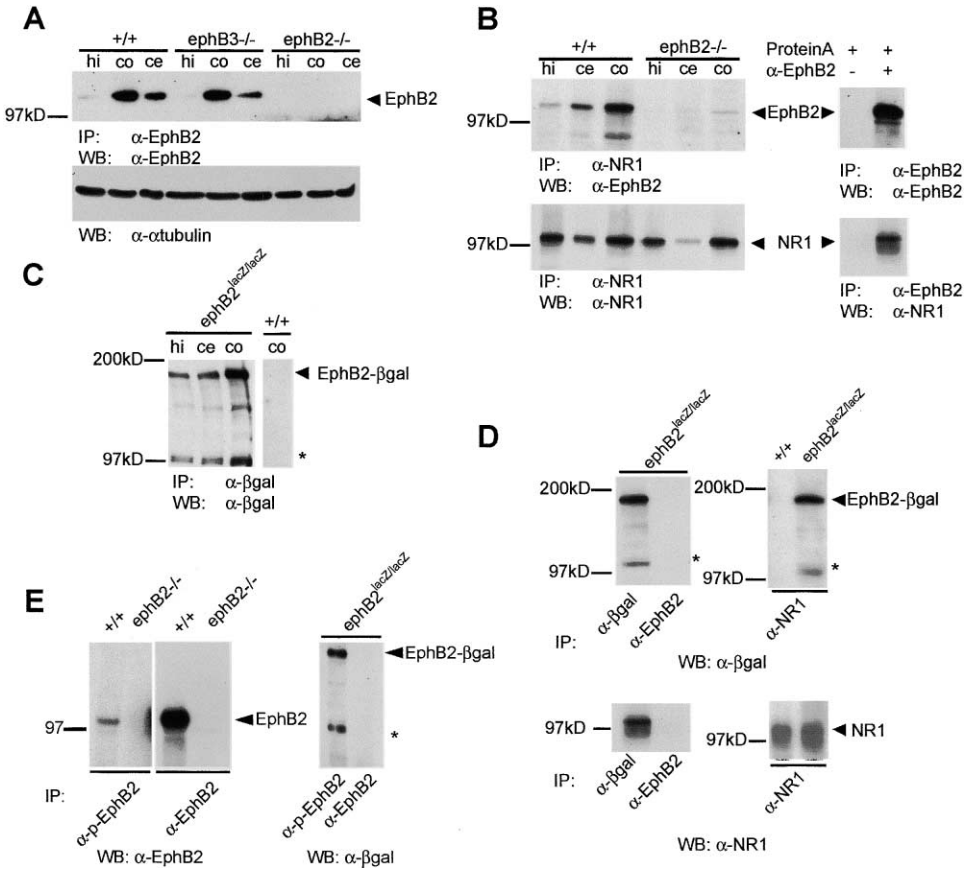

Figure 2. Interaction of EphB2 and EphB2-β-gal with NR1 in Adult Brain

(A) Upper panel: EphB2 protein levels in hippocampus (hi), cerebellum (ce), and cortex (co) of homozygous adult wild-type (+/+), *EphB3*$^{-/-}$, and *EphB2*$^{-/-}$ mice determined by immunoprecipitation using a specific antibody against the SAM domain of EphB2 followed by immunoblotting with the same antibody. Lower panel: Supernatants following EphB2 immunoprecipitation were immunoblotted with anti-α-tubulin to show that similar amounts of protein were loaded.

(B) Coimmunoprecipitation of EphB2 with NR1. Left side: NR1 was immunoprecipitated from either wild-type or *EphB2*$^{-/-}$ brain lysates. Precipitated proteins were immunoblotted with either anti-NR1 (bottom panel) or anti-EphB2 (top panel). EphB2 immunoreactivity is dramatically reduced in *EphB2*$^{-/-}$ brain lysates, the residual signal probably due to cross-reactivity with related EphB receptors. Right side: Immunoprecipitation using either anti-EphB2 or protein A-sepharose beads alone from wild-type brain lysates. Precipitated proteins were immunoblotted with either anti-EphB2 (top panel) or anti-NR1 (bottom panel).

(C) EphB2-β-gal protein was immunoprecipitated from *EphB2*$^{lacZ/lacZ}$ or wild-type (+/+) brain lysates using a specific antibody against β-galactosidase. Precipitated proteins were immunoblotted with the same anti-β-gal antibodies. EphB2-β-gal was specifically detected in *EphB2*$^{lacZ/lacZ}$ tissues and migrated as 190 kDa protein. Asterisk indicates a proteolytically cleaved fragment detected with anti-β-gal.

(D) Left side: Coimmunoprecipitation of EphB2-β-gal with NR1. EphB2-β-gal was immunoprecipitated from *EphB2*$^{lacZ/lacZ}$ brain lysates using anti-β-gal antibodies. Precipitated proteins were immunoblotted with either the same anti-β-gal antibodies (top panel) or anti-NR1 antibodies (bottom panel). Note that EphB2-β-gal is not recognized by immunoprecipitation with anti-(SAM)EphB2 antibodies (top panel). Right side: EphB2-β-gal coimmunoprecipitated with NR1 (bottom panel) when NR1 was immunoprecipitated from *EphB2*$^{lacZ/lacZ}$ cortex (top panel) but not from wild-type tissue using immunoblotting with anti-β-gal.

(E) EphB2-β-gal is tyrosine phosphorylated. Brain lysates from either wild-type (+/+), *EphB2*$^{-/-}$, or *EphB2*$^{lacZ/lacZ}$ mice were subjected to immunoprecipitation with either anti-(SAM)EphB2 or anti-phospho-EphB2 antibodies. Precipitated proteins were immunoblotted with either anti-(SAM)EphB2 (left and middle panels) or anti-β-gal antibodies (right panel). Note that EphB2 and EphB2-β-gal are recognized by anti-phospho-EphB2 antibodies.

2000), and have previously been implicated in NMDA receptor channel activity and synaptic plasticity (Grant et al., 1992; Yu and Salter, 1999). We therefore asked if, in mature and synaptically active neurons, EphB receptor stimulation would lead to an activation of Src family kinases. Similar to the kinetics of ERK and CREB phosphorylation, clustered ephrinB1 markedly increased in vitro Src and Fyn kinase activity (Figure 3E and data not shown). Src family kinases are known to phosphorylate NMDAR subunits on tyrosine residues and increased phosphorylation of NMDAR results in increased channel gating (reviewed in Ali and Salter, 2001). We therefore tested if EphB receptor activation would result in increased tyrosine phosphorylation of NMDAR subunits. Stimulation of cultured neurons with clustered ephrinB1 indeed led to phosphorylation of NR2A subunits after 20 min (Figure 3F). The kinetics of NMDAR phosphorylation were similar to the activation of Src family kinases by EphB receptors (Figure 3E), suggesting an involvement of Src family kinases. However, other pathways downstream of EphB receptors may be involved in phosphorylating NR2A.

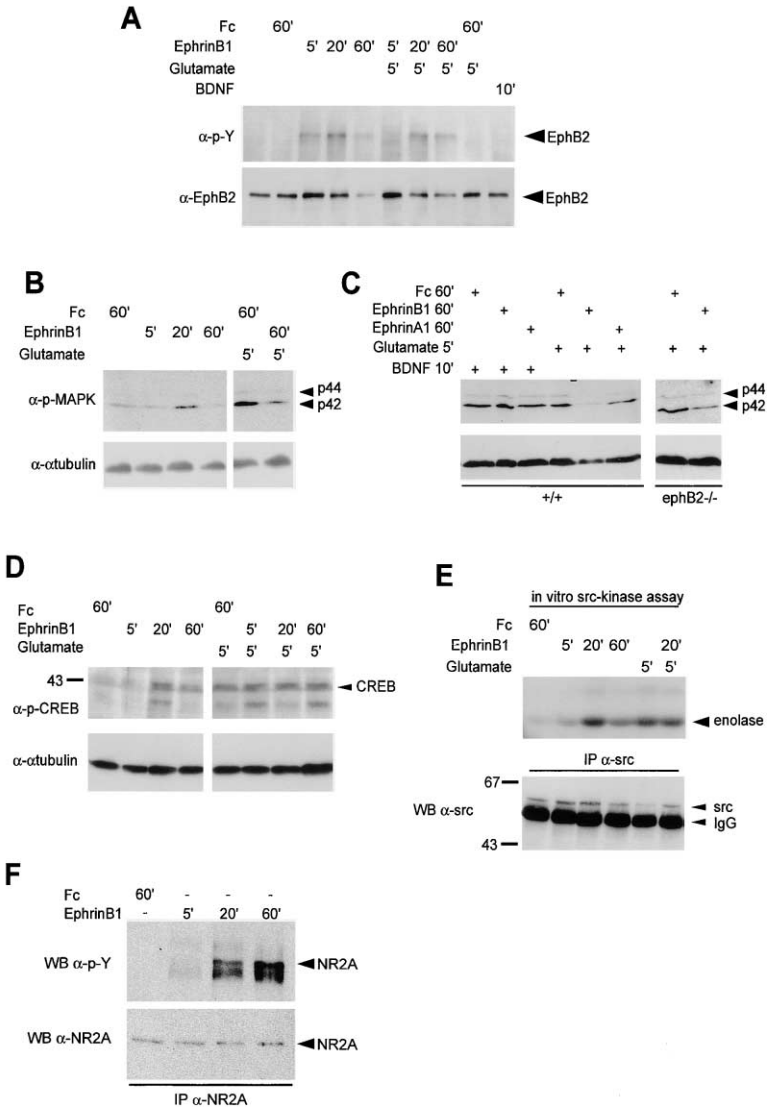

Figure 3. EphB Signaling in Mature Neurons

Cortical and hippocampal neurons were taken from E16.5 wild-type and *EphB2*$^{-/-}$ embryos, dissociated, and cultured for 7 days to allow the formation of synapses.

(A) Cultured neurons were stimulated with either clustered, unfused Fc protein (0.5 μg/ml), clustered ephrinB1-Fc (0.5 μg/ml), glutamate (50 mM), or BDNF (10 ng/ml), either alone or in combination for the indicated times. Cells were lysed and EphB2 protein immunoprecipitated using anti-(SAM)EphB2. Autophosphorylation of EphB2 was visualized by immunoblotting with a phosphotyrosine-specific antibody (4G10). The stripped blot was subsequently reprobed with anti-(SAM)EphB2 to determine the levels of EphB2 protein in the IPs. Note that costimulation with glutamate and ephrinB1-Fc did slightly delay ephrinB1-Fc-induced EphB2 autophosphorylation at the earliest time point. Prolonged ephrinB1-Fc stimulation caused receptor degradation.

(B) Stimulation of hippocampal neurons with clustered ephrinB1-Fc caused the formation of phosphorylated p42ERK with delayed kinetics (20 min, top panel), as shown by immunoblotting of whole-cell lysates with phosphospecific MAPK antibodies. Stimulation with glutamate (in the presence or absence of unfused Fc protein [data not shown]) led to the rapid (5 min) accumulation of higher levels of phosphorylated p42ERK. Preincubation with clustered ephrinB1-Fc (60 min) strongly suppressed glutamate-induced phosphorylation of p42ERK. Stripped blot was immunoblotted with anti-α-tubulin antibodies to visualize amounts of protein loaded on the gel.

(C) Left panel: Stimulation of cortical and hippocampal neurons from wild-type embryos with BDNF (10 ng/ml) led to a strong increase in active MAPK that could not be suppressed by costimulation with ephrinB1-Fc (0.5 μg/ml) or ephrinA1-Fc (0.5 μg/ml). Note that glutamate-induced MAPK is partially inhibited by costimulation with ephrinA1-Fc but remains still stronger than when costimulated with ephrinB1-Fc. Right panel: *EphB2*$^{-/-}$ neurons show a very similar behavior compared to wild-type controls. Again, costimulation with glutamate and ephrinB1-Fc significantly decreased glutamate-activated MAPK. (D) Stimulation of hippocampal and cortical neurons with clustered ephrinB1-Fc caused the formation of phosphorylated CREB protein with delayed kinetics (20 min, top panel) as compared to glutamate (5 min), as shown by immunoblotting of whole-cell lysates with phosphospecific CREB antibodies. In contrast to phosphorylated p42ERK, preincubation with clustered ephrinB1-Fc did not suppress glutamate-induced phosphorylation of CREB. Stripped blot was immunoblotted with anti-α-tubulin antibodies to visualize amounts of protein loaded on the gel.

(E) Stimulation of hippocampal and cortical neurons with clustered ephrinB1-Fc led to an increase in in vitro Src kinase activity toward the exogenous substrate enolase. The kinetics of Src activation was similar to the phosphorylation of p42ERK and CREB. Stimulation with glutamate also increased Src kinase activity. The effect was not further increased by costimulation with ephrinB1-Fc.

(F) EphB receptor stimulation with clustered ephrinB1-Fc led to phosphorylation of NR2A subunits of the NMDA receptor in cultured hippocampal and cortical neurons. Phosphorylation of NR2A was detected at 20 min of stimulation by immunoprecipitation of NR2A and immunoblotting with an antibody to detect phosphorylated tyrosine residues (upper panel). Subsequently, the blot was stripped and reprobed with an antibody to visualize levels of NR2A protein (lower panel). Note similar kinetics of Src activation and onset of NR2A phosphorylation.

Changes in Synapse Numbers and EphB/NR1 Coclusters in EphB2-Deficient Mice

Given that EphB2 interacts with and possibly regulates NMDA receptor function, we next analyzed NMDA receptor-dependent synaptic plasticity in *EphB2*$^{-/-}$ and *EphB2*$^{lacZ/lacZ}$ mice. In selected experiments, we included *EphB3*$^{-/-}$ mice, because, during development, EphB3 synergizes with EphB2 in the formation of commissures (Cowan et al., 2000; Orioli et al., 1996). To distinguish between defects caused by aberrant morphologies or by altered signaling at synapses, we investigated adult hippocampal structure. Control, *EphB2*$^{-/-}$, *EphB2*$^{lacZ/lacZ}$, and *EphB3*$^{-/-}$ brains were analyzed by Nissl and immunostaining using markers for neuronal processes and subpopulations. No significant alterations in cell numbers and processes were observed, except for an apparent, mild reduction in cell density in the CA1 region of *EphB3*$^{-/-}$ mice (see supplemental data at http://www.neuron.org/cgi/content/full/32/6/1027/DC1). At the ultrastructural level, we observed normal morphology of CA1 synapses in all mutants, including the size of the synaptic cleft, and pre- and postsynaptic specializations

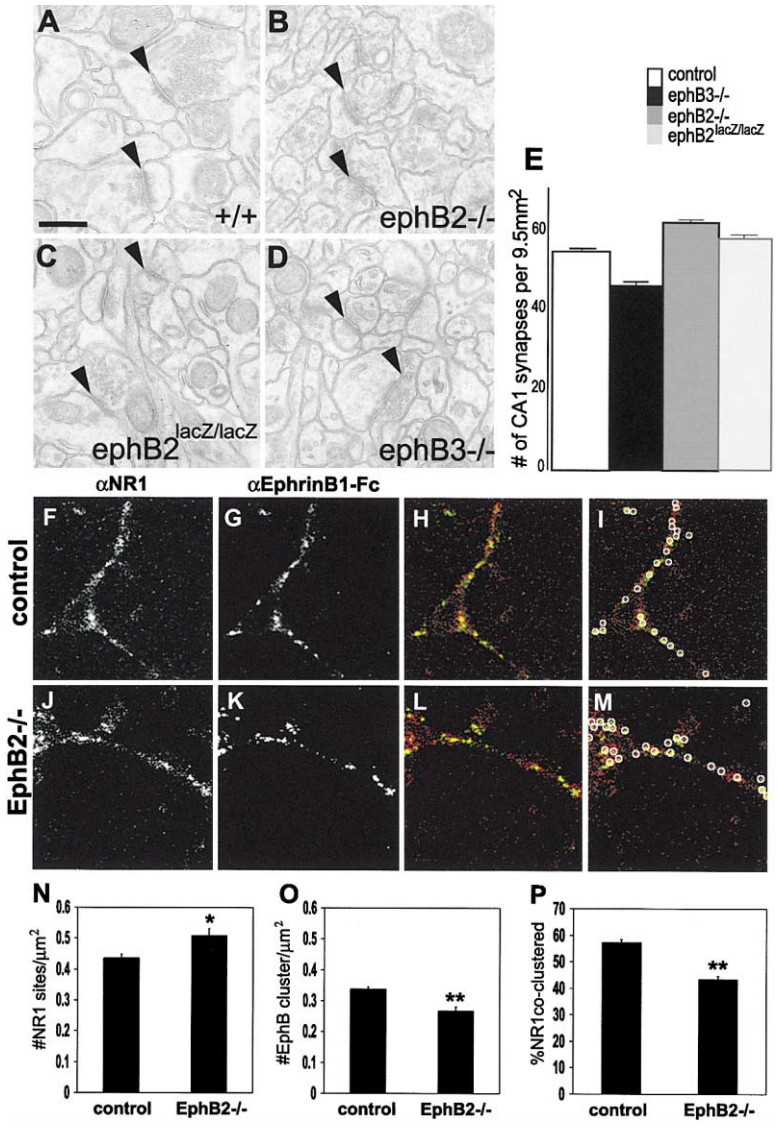

Figure 4. Morphological Analysis of Synapses in the CA1 Region of Wild-Type and Mutant Mice

(A–D) Ultrastructural analysis of synaptic morphology in CA1 stratum radiatum showing normal asymmetric morphology of synapses in wild-type (A), *EphB2*$^{-/-}$ (B), *EphB2*$^{lacZ/lacZ}$ (C), and *EphB3*$^{-/-}$ (D) mice.

(E) Numbers of synapses per 9.5 mm^2 in the CA1 region of wild-type and mutant hippocampi. Note a small, but significant reduction in *EphB3*$^{-/-}$ mice ($p < 0.0001$) and a small, but significant increase in *EphB2*$^{-/-}$ mice ($p < 0.0001$), and no changes compared to control samples in *EphB2*$^{lacZ/lacZ}$ mice. Scale bar: 0.8 μm.

(F–P) Fluorescence analysis of NR1 clustering in cultured hippocampal and cortical neurons. Cells were derived from *EphB2*$^{-/-}$ and wild-type littermates at E16.5 and stimulated with clustered ephrinB1-Fc (2 μg/ml) for 1 hr. (F) and (J) show NR1 sites visualized with an anti-NR1 antibody. (G) and (K) show immunofluorescent detection of clustered ephrinB1-Fc presumably bound to EphB receptor sites. (H) and (L) show the overlay. (I) and (M) show an example of the computer-based quantification of coclustered NR1 sites with EphB receptors. (N–P) NR1 and EphB sites were counted per cell, and the coclusters were quantified using a computer program ($n = 89$ and 82 cells for control and *EphB2*$^{-/-}$, respectively). (N) The number of NR1 sites per μm^2 is significantly increased in the *EphB2*$^{-/-}$ ($p = 0.0065$). (O) Less EphB receptor clusters were counted in the *EphB2*$^{-/-}$ compared to control ($p < 0.0001$) (P) The percentage of NR1 subunits coclustered with EphB receptors is significantly reduced in the *EphB2*$^{-/-}$ ($p < 0.0001$).

(Figures 4A–4D). Interestingly, we revealed mild changes in synaptic numbers in the CA1 region of the hippocampus. Micrographs from *EphB3*$^{-/-}$ animals showed a slight, yet significant reduction of synapses compared to controls (Figure 4E; $n = 3$ and 6 animals, respectively; $n > 1000$ synapses counted/animal, $p = 0.0001$), possibly a consequence of the reduced cell density in the CA1 region of EphB3-deficient hippocampi. In contrast, *EphB2*$^{-/-}$ mice showed a slight, but significant *increase* in the number of synapses compared to controls (Figure 4E; $n = 3$ and 6 animals, respectively; $n > 1000$ synapses counted/animal, $p = 0.0001$). No significant changes in the number of synapses were found in *EphB2*$^{lacZ/lacZ}$ mice, indicating that the changes in *EphB2*$^{-/-}$ mice were independent of the kinase domain of the receptor.

We next asked if lack of EphB2 would alter the distribution and number of NMDA receptor sites in cultured neurons. Mixed hippocampal and cortical neuron cultures were established from individual embryos derived from intercrosses of *EphB2* heterozygotes and stimulated after 1DIV with ephrinB1-Fc (60 min). EphB/NR1 coclusters were visualized by costaining against NR1 and ephrinB1-Fc and quantified using NIHImage software counting single receptor sites and colocalized EphB/NR1 clusters. Despite the significant functional redundancy between EphB receptors (Dalva et al., 2000), we detected modest yet significant changes in *EphB2*$^{-/-}$ neurons compared to +/+ controls. The number of EphB clusters (stained with ephrinB1-Fc) decreased slightly (20%) in *EphB2*$^{-/-}$ neurons, indicating the presence of other EphB receptors binding to ephrinB1-Fc (Figure 4O). The number of EphB/NR1 coclusters decreased by a similar margin (20%, Figure 4P), concomitant with a slight increase in the number of NR1 sites (stained with anti-NR1) in *EphB2*$^{-/-}$ neurons (15%, Figure 4N). These findings suggest that in *EphB2*$^{-/-}$ mice a significant fraction of NR1 receptors no longer coclustered with EphB receptors and encouraged us to investigate whether there may also be defects in activity dependent synaptic plasticity in these mice.

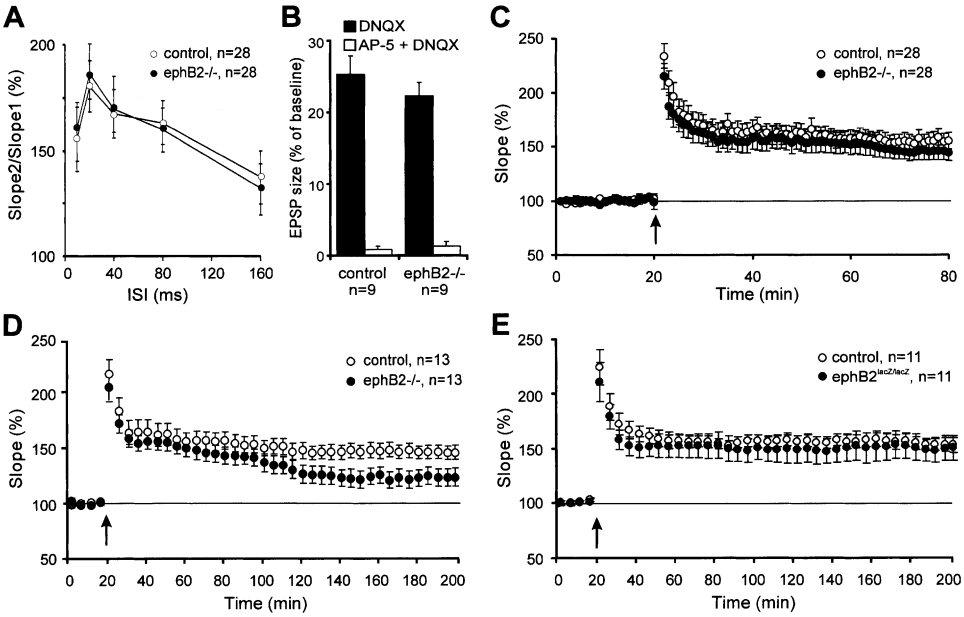

Figure 5. Hippocampal Long-Term Potentiation Is Modestly Reduced in *EphB2*$^{-/-}$ Mutants

(A) Control wild-type slices (open circles, n = 28 from eight mice) and *EphB2*$^{-/-}$ slices (closed circles, n = 28 from eight mice) show normal paired-pulse facilitation of the fEPSP at various interstimulus intervals (ISI). Error bars: SEM.

(B) NMDA responses are normal in *EphB2*$^{-/-}$ mice at CA1 pyramidal cells. After 15 min of baseline stimulation in normal ACSF, 10 μM DNQX was added for 15 min (with low Mg^{2+} and high Ca^{2+}, see Experimental Procedures). Average responses were taken 10–15 min after beginning of DNQX application. The remaining response was reduced to zero after additional application of 50 μM AP-5. NMDA-responses are slightly higher in controls, but the difference is not significant ($p > 0.05$, t test). Error bars: SEM, n = number of slices from four mice per animal group.

(C) E-LTP is normal in *EphB2*$^{-/-}$ mice at the CA3-CA1 pyramidal cell synapse. As long as 60 min after theta-burst stimulation (TBS, closed arrow), the fEPSP from control (n = 28 slices from eight mice) and *EphB2*$^{-/-}$ (n = 28 slices from eight mice) slices were not significantly different. There is, however, a small decrease in the *EphB2*$^{-/-}$ signal in comparison to control slices over time. Error bars: SEM.

(D) L-LTP of wild-type and *EphB2*$^{-/-}$ mice is significantly different. In a new set of experiments, recordings from CA3-CA1 pyramidal cell synapses in the hippocampus were recorded for 3 hr after theta-burst stimulation (closed arrow). 170–180 min after TBS, the average potentiation for control slices was 145.8% ± 8.6% (n = 13 slices from four mice) and 122.7% ± 9.1% for the *EphB2*$^{-/-}$ mice (n = 13 slices from four mice). This difference is significant ($p = 0.03$, t test).

(E) L-LTP in *EphB2*$^{lacZ/lacZ}$ is normal compared to control mice. The average degree of potentiation 170–180 min after TBS was 152.4% ± 6.5% for the control mice (n = 11 slices from four mice) and 149.6% ± 11.6% for the *EphB2*$^{lacZ/lacZ}$ mice (n = 11 slices from four mice). The difference between the two groups was not significant ($p > 0.1$, t test). Error bars: SEM.

EphB2-Deficient Mice Show Modestly Reduced Hippocampal Long-Term Potentiation

Before investigating long-term changes in synaptic plasticity, we analyzed wild-type and mutant mice with respect to basal synaptic transmission. To compare the average synaptic responses to baseline stimulation, we averaged five sweeps during baseline stimulation in hippocampal slices from *EphB2*$^{-/-}$ mice and wild-type mice and found no significant differences in average fEPSP (field excitatory postsynaptic potential) amplitude (see supplemental data). We measured paired-pulse facilitation (PPF) by applying two stimuli separated by different time intervals and recorded the evoked fEPSPs. Figure 5A shows the increase in fEPSP slope of the second relative to the first fEPSP. At all tested intervals, the values for control and *EphB2*$^{-/-}$ mice were not significantly different ($p > 0.3$, t test, Figure 5A). Also, the difference in post tetanic potentiation (PTP) after theta burst stimulation (TBS) between the genotypes was not significant (data not shown; $p = 0.29$; t test). We compared the size of the presynaptic fiber volley (PSFV), which is proportional to the number of presynaptic fibers recruited by electric stimulation, with the slope of the fEPSP to provide an accurate indication of basal synaptic transmission. Furthermore, stimulus-response curves were measured in both mutants and compared to wild-type (see supplemental data). In both these respects, we found that basal synaptic transmission was normal in *EphB2*$^{-/-}$ and in *EphB2*$^{lacZ/lacZ}$ mice (see supplemental data). To measure the NMDA-component of the EPSP signal, we recorded wild-type and *EphB2*$^{-/-}$ slices in the presence of the AMPA receptor antagonist DNQX (in low Mg^{2+} ACSF). Mutant slices showed a trend toward a reduced NMDA receptor component. However, the difference was marginal (and also not statistically significant) (Figure 5B). The NMDA component of the fEPSP was reduced to zero when AP-5 (50 μM) was applied together with DNQX. Similar results were obtained for the fEPSP slope and the integral for the whole fEPSP signal (data not shown). In summary, all electrophysiological experiments revealed no significant changes in basal synaptic transmission in *EphB2*$^{-/-}$ mice.

We next measured CA3-CA1 LTP in hippocampal slices of *EphB2*$^{-/-}$ mice after TBS, which is known to be an efficient stimulus to induce LTP (Bliss and Col-

lingridge, 1993). All experiments were performed in a strictly blinded fashion, and the genotypes of the mice were only revealed after the final data analysis. Figure 5C shows the summary graph for all E-LTP recordings. Both groups show clear LTP with no obvious difference between genotypes. The average degree of potentiation 55–60 min after TBS relative to baseline mean (100%) was 146.0% ± 6.6% for the *EphB2*$^{-/-}$ mice (n = 28 slices from eight mice) and 154.1% ± 9.7% for the wild-type siblings (n = 28 slices from eight mice; p = 0.51, t test). 75% of control slices showed successful LTP, compared to 68% of *EphB2*$^{-/-}$ slices. Since there was a tendency for LTP in *EphB2*$^{-/-}$ slices to decline more rapidly than control slices (Figure 5C), we performed a new series of experiments to analyze long-lasting LTP (L-LTP). In this set, *EphB2*$^{-/-}$ mice again showed normal PTP and normal E-LTP, but the EPSP slope became significantly different compared to wild-type slices starting 100 min after TBS application (Figure 5D). The average degree of potentiation 170–180 min after TBS was 122.7% ± 9.1% for the *EphB2*$^{-/-}$ mice (n = 13 slices from four mice) and 145.8% ± 8.6% for the wild-type siblings (n = 13 slices from four mice). The difference between the two groups was significant (p = 0.03, t test). 69% of control slices showed successful L-LTP compared to 38.5% in *EphB2*$^{-/-}$ slices. Interestingly, *EphB2*$^{lacZ/lacZ}$ mice showed normal L-LTP, in contrast to *EphB2*$^{-/-}$ mice (Figure 5E). The average degree of potentiation 170–180 min after TBS was 152.4% ± 6.5% for the control mice (n = 11 slices from four mice) and 149.6% ± 11.6% for the *EphB2*$^{lacZ/lacZ}$ mice (n = 11 slices from four mice). The difference between the two groups was not significant (p > 0.1, t test).

Long-Term Synaptic Depression Is Blocked in *EphB2*$^{-/-}$ Mice, but Rescued in *EphB2*$^{lacZ/lacZ}$ Mice

To test if also other forms of plasticity were affected, we analyzed hippocampal LTD and depotentiation in the CA3-CA1 pathway of wild-type and *EphB2*$^{-/-}$ mice. After recording stable baseline responses (see Experimental Procedures), LTD was induced by low-frequency stimulation (LFS) of 900 stimuli at 1 Hz (15 min). Figure 6A shows a summary graph of all LTD experiments. Both groups were indistinguishable during LFS and the initial phase of LTD, but shortly thereafter the two curves separated. Whereas slices of wild-type mice continued to show LTD, *EphB2*$^{-/-}$ slices quickly returned to baseline levels. To quantify the amount of LTD for the two groups, we calculated the mean fEPSP slope. Whereas 55–60 min after LFS, wild-type mice exhibited a reduction of fEPSP-slope to 83.1% ± 4.3% (n = 14 slices from four mice) of the baseline average, *EphB2*$^{-/-}$ mice returned to 95.0% ± 3.6% (n = 20 slices, seven mice; p = 0.0033, t test). To compare the probability of successful LTD induction between the two groups, we scored a reduction of fEPSP slope to less than 90% of baseline average 55–60 min after LFS as successful LTD. According to this criterion, LTD occurred in 78.5% of all wild-type recordings (11 out of 14 slices), whereas in the knockout animals LTD was only maintained in 35% for all recordings (7 out of 20 slices).

To analyze depotentiation, we first recorded a baseline and then applied a TBS to induce LTP, followed after 10 min by a depotentiation stimulus (LFS of 900 stimuli at 1 Hz for 15 min). Wild-type and *EphB2*$^{-/-}$ slices showed a normal initiation phase of LTP (first 10 min after TBS application), and depotentiation followed 15 min of 1 Hz stimulation. However, *EphB2*$^{-/-}$ slices were

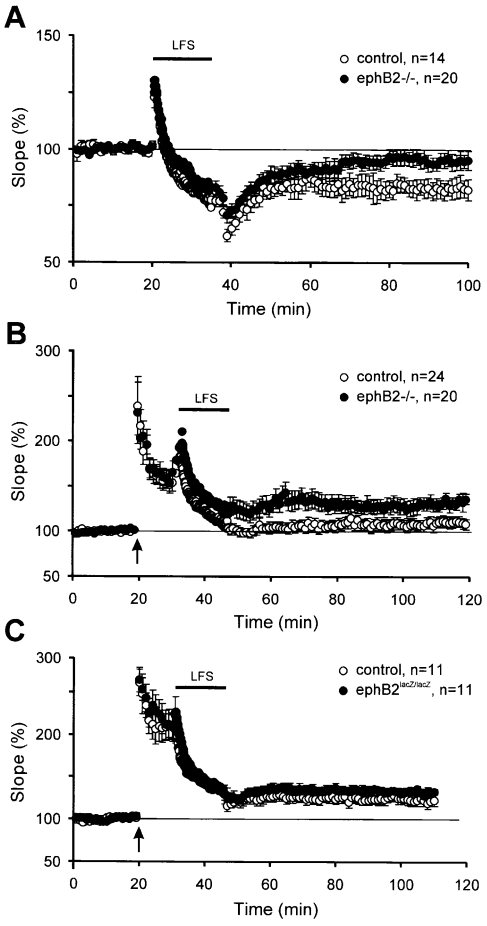

Figure 6. Synaptic Depression Is Blocked in *EphB2*$^{-/-}$ Mutants, but Rescued in *EphB2*$^{lacZ/lacZ}$ Mice

(A) Hippocampal long-term depression (LTD) is defective in *EphB2*$^{-/-}$ mutants. Low-frequency stimulation (LFS, closed bar) produced a reduction in the initial phase of the fEPSP in slices from control wild-type mice 55–60 min after LFS: 83.1% ± 4.3% (n = 14 slices from four mice) but not from *EphB2*$^{-/-}$ mice (95.0% ± 3.6%, n = 20 slices, seven mice). This difference is highly significant (p = 0.0033, t test). Error bars: SEM.

(B) Depotentiation is impaired in *EphB2*$^{-/-}$ mutants. 10 min after TBS (closed arrow) to produce the initial phase of LTP, slices were subjected to a 15 min LFS train (closed bar, 1 Hz). The fEPSPs from control slices (n = 24 slices from six mice) returned almost to baseline (110.5% ± 6.1%), whereas *EphB2*$^{-/-}$ slices (n = 20 slices from five mice) were not persistently depotentiated (132.9% ± 7.0%). The difference between wild-type and *EphB2*$^{-/-}$ mice is highly significant (p = 0.0023, t test).

(C) Depotentiation is rescued in *EphB2*$^{lacZ/lacZ}$ mice. Using the same protocol as in (B), we could not observe a significant difference in depotentiation from *EphB2*$^{lacZ/lacZ}$ mice in comparison to wild-type siblings. The fEPSPs from control slices (n = 11 slices from three mice) returned was depotentiated to (122.8% ± 6.4%), whereas *EphB2*$^{lacZ/lacZ}$ slices (n = 11 slices from three mice) were not persistently depotentiated (132.3% ± 5.1%). The difference between wild-type and *EphB2*$^{lacZ/lacZ}$ mice is not significant (p > 0.1, t test).

depotentiated to a much lesser degree than control slices (Figure 6B). 55–60 min after LFS application, control slices (n = 24 slices from six mice) showed on the average a 110.5% ± 6.1% fEPSP slope size (in comparison to the first 20 min of baseline recording), whereas *EphB2*$^{-/-}$ mice (n = 20 slices from five mice) showed a less depotentiated fEPSP size compared to control slices (132.9% ± 7.0%). This difference was highly significant ($p = 0.0023$, t test).

We next asked if the presence of the truncated EphB2-β-gal fusion protein would rescue this defect as it did in the case of L-LTP. Figure 6C shows that when treated with the same protocol, *EphB2*$^{lacZ/lacZ}$ mice showed normal depotentiation, indistinguishable from their control littermates. 55–60 min after LFS stimulation, control slices (n = 11 slices from three mice) showed on the average a 122.8% ± 6.4% fEPSP slope size (in comparison to the first 20 min of baseline recording), and *EphB2*$^{lacZ/lacZ}$ mice (n = 11 slices from three mice) showed a fEPSP size of 132.3% ± 5.1%. This was not significant ($p > 0.1$, t test). It should be noted that, in this series of experiments, the initial phase after TBS stimulation showed a higher degree of potentiation than for the depotentiation experiments of the *EphB2*$^{-/-}$ mice (Figure 6B, 20 t, 20 min). In summary, these findings indicate a severe defect of *EphB2*$^{-/-}$ mice in depotentiation, which was rescued in *EphB2*$^{lacZ/lacZ}$ mice, suggesting that this function was again independent of EphB2 kinase activity.

Lack of EphB2 Causes Behavioral Defects, which Are Rescued by Truncated EphB2

Given the expression of EphB2 in the hippocampus and the defects in signaling and activity-dependent synaptic plasticity in *EphB2*$^{-/-}$ mice, we set out to examine these mice for potential behavioral defects and, in particular, asked whether the observed defects in synaptic plasticity would translate into defects in learning and memory. While *EphB2*$^{-/-}$ mutants do exhibit defects in the formation of forebrain commissures (Orioli et al., 1996), we suggest it is unlikely that these anatomical defects would perturb behavior in learning assays, since similar defects in humans do not apparently produce learning and memory abnormalities (Meyer et al., 1998). Neither *EphB2*$^{-/-}$ nor *EphB2*$^{lacZ/lacZ}$ mice exhibited obvious deficiencies in life span and physical parameters such as general fitness and motor control (data not shown). In the open field, *EphB2*$^{-/-}$ and *EphB2*$^{lacZ/lacZ}$ mutants exhibited mildly increased activity compared to their wild-type littermates (data not shown) in part due to decreased habituation (familiarization with unknown territory). To assess hippocampus-dependent learning performance, we tested *EphB2*$^{-/-}$ mice in the Morris water maze (Morris, 1982). In this task, mice have to swim in opaque water and learn, using extramaze visual cues, to find a platform hidden beneath the water surface. With the experimenter blind with respect to genotype, mice were trained for 18 trials followed by 12 trials reversal with the platform in a new position. *EphB2*$^{-/-}$ animals consistently required more time and longer swim paths to find the hidden platform (ANOVA genotype, $p = 0.0001$; Figure 7A). *EphB2*$^{-/-}$ mice were already impaired during the very first trial, suggesting that they had trouble mastering the early adaptation to the test. During the reversal phase, when the platform was moved to a new position, knockouts as well as controls required more time to reach the platform (Figure 7A; trial block 10, two-way ANOVA reversal effect, $p = 0.0008$; interaction reversal effect, genotype nonsignificant), suggesting that both groups had previously adapted their escape strategy to the specific platform position. However, while controls spent significantly more time in the former goal quadrant than in adjacent quadrants (ANOVA place, $p < 0.0030$), *EphB2*$^{-/-}$ mice did not (ANOVA place, nonsignificant; two-way ANOVA interaction genotype place, $p = 0.1017$; Figure 7C). During visible platform training (platform marked with a flag and moved to a new position for each trial) *EphB2*$^{-/-}$ animals had again difficulties in adapting to the new test situation, resulting in a large variability of initial performance (Figure 7A; trial block visible). Eventually, however, performance of all *EphB2*$^{-/-}$ animals became indistinguishable from controls (two-way ANOVA genotype, $p = 0.0553$; interaction genotype trial block, $p = 0.0377$), establishing that they were able to process visual information. Together, these results point to a subtle requirement for EphB2 in maze performance. However, a number of confounds make these results difficult to interpret, with respect to a potential role for EphB2 in hippocampal-dependent learning. First, *EphB2*$^{-/-}$ mice were already impaired during the very first trial, suggesting that they had trouble mastering the early adaptation to the test. In addition, slightly reduced swim speed and an increased tendency of some animals for passive floating (data not shown) contributed to the reduced escape performance of *EphB2*$^{-/-}$ mice, making it difficult to distinguish between a mild impairment in hippocampus-dependent learning and a more general performance deficit. While ultimately the cause of the behavioral defects in these mice remains unclear, we found that these defects, whatever their source, were rescued in the *EphB2*$^{lacZ/lacZ}$ mice. Unlike *EphB2*$^{-/-}$ mice, *EphB2*$^{lacZ/lacZ}$ mice were indistinguishable from controls during both acquisition and reversal learning with respect to all measures of escape performance (Figure 7B). *EphB2*$^{lacZ/lacZ}$ mutants spent significantly more time in the former goal quadrant than in the other quadrants (ANOVA place, $p = 0.0001$) during the probe trial (Figure 7C, right panel). The results from the *EphB2*$^{lacZ/lacZ}$ mice indicate that this function is independent of EphB2 kinase signaling.

Discussion

In this study, we made four important findings. First, Eph receptor activation in cultured forebrain neurons regulates signaling pathways implicated in synaptic plasticity, suggesting cross-talk of EphB2/NMDAR signaling pathways. Second, lack of EphB2/NMDA receptor interaction did not result in obvious changes in synapse morphology. Third, lack of EphB2 impaired long-lasting LTP and completely extinguished LTD and depotentiation. And, fourth, targeted expression of the truncated EphB2-β-gal fusion protein rescued plasticity and behavioral defects, indicating that EphB2 exerts its functions in a kinase-independent manner.

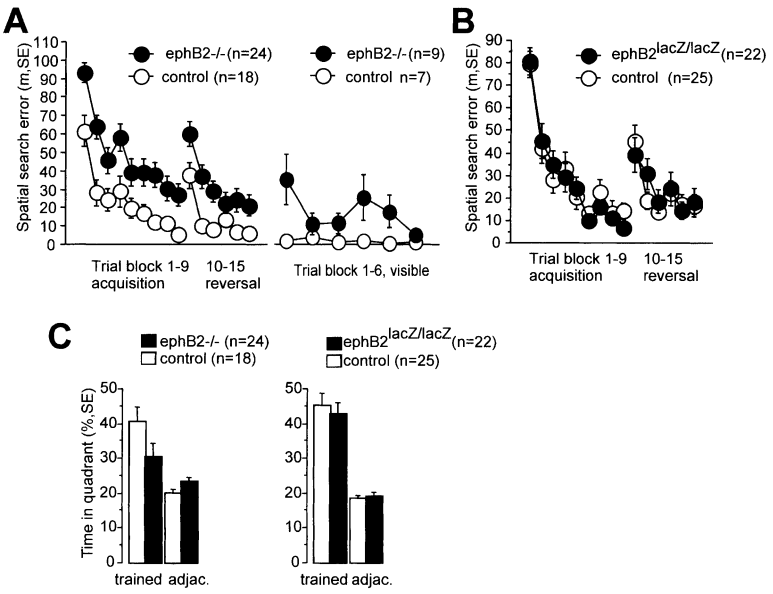

Figure 7. Behavior of *EphB2* Mutant Mice in Hippocampus-Dependent Learning Tasks

(A–C) Spatial memory task—Morris water maze.

(A) Left graph: Acquisition phase during invisible version. Spatial search error displays the mean distance the subject has from the goal platform calculated every 0.15 min of swum distance (Gallagher et al., 1993). Mice were trained for 18 trials (trial block 1–9) spread over 3 consecutive days (six trials per day), followed by 2 days of reversal phase with the platform at the opposite position in the pool (trial block 10–15 reversal). *EphB2*$^{-/-}$ mice ($n = 24$) showed an increase in spatial search errors compared to littermate controls ($n = 18$; $p = 0.0006$). Right graph: 2 days of visible version of the water maze. Both *EphB2*$^{-/-}$ and control mice show much reduced spatial search errors.

(B) Spatial learning of *EphB2*$^{lacZ/lacZ}$ mice during the acquisition phase of the invisible version of the water maze.

(C) Probe trials (trial 19, first trial of reversal phase) expressed as percent time spent in the quadrant around the former goal or control zone. Chance level is 25%. Mutants and control group show significant spatial learning. Note that *EphB2*$^{-/-}$ animals spent significantly less time in the trained quadrant compared to controls ($p = 0.0003$) (left), whereas *EphB2*$^{lacZ/lacZ}$ mice spent about the same time in the trained quadrant as littermate controls. ($p = 0.6321$) (right).

Signaling by Synaptic Ephrins and Ephs

The recent observation that EphB2 receptors and the NR1 subunits of NMDA receptors interacted in primary embryonic neurons and that continued exposure to ephrinB increased the number of synapses in culture (Dalva et al., 2000) suggested that Eph receptors play a role in synapse formation and/or that the EphB2/NR1 complex would somehow influence downstream signaling at the synapse. While our findings confirm direct EphB2/NR1 interactions, they also suggest additional indirect cross-talk. ERK/MAP kinases play important roles in vertebrate and invertebrate neuronal plasticity and memory formation (reviewed in Impey et al., 1999). ERK/MAPKs may be activated downstream of NMDA channel-mediated Ca^{2+} influx and subsequent activation of Ca^{2+}-dependent RasGEFs. Targets of ERK/MAPKs in synaptic plasticity include CAMs, cytoskeletal elements, and CREB. We show that EphB receptor activation in cultures of hippocampal neurons leads to a modest phosphorylation of ERK/MAPKs and CREB with delayed kinetics (20 min). Conversely, long-term stimulation (60 min) of EphB receptors with clustered ephrinB ligand counteracted glutamate-activated MAPK activity. The time course of this effect correlates with the kinetics of coclustering of EphB2 with NR1 suggesting that direct association may be involved. Activation of A-type Eph receptors, which appear not to directly interact with NMDAR (Dalva et al., 2000) led to a partial inhibition of glutamate-induced ERK phosphorylation suggesting that Eph receptors counteract the ERK pathway indirectly and more distally perhaps via recruitment of RasGAP (for review, see Wilkinson, 2000). Inhibition of ERK phosphorylation by EphA receptors was recently demonstrated in nonneuronal cells in response to a variety of stimuli (Miao et al., 2001). ERKs may also provide the biochemical link to EphB2-regulated long-term depression, since they were recently shown to be required for cerebellar LTD (Kawasaki et al., 1999).

In contrast to ERKs, glutamate-activated CREB phosphorylation was not suppressed by ephrinB, suggesting that glutamate induces CREB phosphorylation via separate pathways. Ca^{2+}-dependent protein kinases are crucially involved in CREB phosphorylation, and CaMKIV is a likely candidate. Mice lacking CREB (Bourtchuladze et al., 1994) or expressing a dominant-negative form of CamKIV (thereby having reduced levels of phospho-CREB) (Kang et al., 2001) display deficiencies in L-LTP but not in E-LTP. Similar effects were seen in *EphB2*$^{-/-}$ mice (this study), suggesting that CREB is an important downstream target of EphB2.

Stimulation of cultured neurons with clustered ephrinB1 elicited activation of Src tyrosine kinase. Src family kinases are essential players in LTP and learning and memory (Grant et al., 1992; Yu and Salter, 1999). Src is part of the NMDA receptor protein complex (Husi et al., 2000) and may potentiate NMDA channel activity by phosphorylating the NR2 subunits (Yu and Salter, 1999; reviewed by Ali and Salter, 2001). It is possible that EphB2-mediated Src family kinase activation enhances NMDA channel activity and therefore contributes to the maintenance of the late phase of LTP. In fact, induction of EphB/NMDAR association in cultured neurons stimulates tyrosine phosphorylation of the NMDA receptor (this study) and leads to a large increase in the ability of the NMDA receptor to flux Ca^{2+} in response to glutamate (Takasu et al., 2002). Whether Src family kinases also play a role in the regulation of long-term depression is not known. Alternatively, Src tyrosine kinases may contribute to the regulation of cytoskeleton dynamics (reviewed in Bjorge et al., 2000) and may represent important downstream effectors of EphB-mediated actin reorganization. Src family kinases may also regulate

NMDAR function downstream of ephrin ligands. Our in situ hybridization analysis showed that at least with respect to the CA3-CA1 pathway, ephrinB ligands are expressed in postsynaptic CA1 neurons, rather than in presynaptic CA3 cells. This suggests that in adult CA3-CA1 hippocampal synapses ephrinB ligands might be coexpressed with EphB2 receptors on the postsynaptic side, perhaps in complexes involving NMDA receptors. Stimulation of ephrinB by soluble EphB-Fc proteins induces the activation of Src family kinases in cultured excitatory neurons (A. Palmer, M. Zimmer, K. S. Erdmann, A. Porthin, R. Heumann, U. Deutsch, and R.K., unpublished data). This raises the possibility that postsynaptic ephrinB proteins may contribute to Src family kinase-mediated potentiation of NMDA channel activity and that postsynaptic EphBs might play a modulatory role. Whether the interaction between ephrinB and EphB occurs in *trans*, i.e., presynaptic EphB interacting with postsynaptic ephrinB, or in *cis*, i.e., both proteins interacting on the postsynaptic side, remains to be investigated.

EphB2/NR1 Coclusters: Regulators of Synaptogenesis or Synapse Function?

Our histological analyses of *EphB2* and *EphB3* mutant mice did not reveal major defects in hippocampal synapse morphology (nor in the general architecture and connectivity) indicating that EphB receptors are not the primary organizers of excitatory synapses. This in itself was not terribly surprising, since synapses lacking the PDZ domain scaffolding protein PSD-95 showed normal synaptic morphology (Migaud et al., 1998) and may simply reflect a high degree of redundancy in this system. We did observe that in the absence of EphB2, young cultured neurons did not display reduced numbers of NR1 sites (to the contrary, the numbers of NR1 sites slightly increased in *EphB2*$^{-/-}$ neurons), but a significant proportion of those NR1 sites lacked association with EphB receptors, when cells were stimulated with ephrinB. This fraction of NMDAR may not be regulated by Src and may be functionally impaired in vivo, providing an explanation for the plasticity defects in *EphB2*$^{-/-}$ mice (see below). It may further explain the interesting effect EphB mutations had on synapse numbers. Cells with reduced NMDA receptor channel activity may compensate by increasing the numbers of synapses (as observed for *EphB2*$^{-/-}$ mice). Alternatively, EphB2 receptors may play a role in synapse elimination in young animals, a process that has been correlated with LTD in the cerebellum (Kano et al., 1995). In addition, EphB receptors may be involved in regulating structural proteins at synapses, including PDZ domain proteins (Buchert et al., 1999), cell adhesion molecules (CAMs), and integrins (reviewed in Drescher, 2000). Lack of EphB receptors may stabilize or destabilize synapses depending on the activity state of the synapse and the molecular environment at the postsynaptic density.

Changes in Hippocampal Plasticity

The association between EphB2 and NMDA receptors may not regulate major structural changes at the synapse but may lead to changes in functional properties of these proteins and to changes in synaptic plasticity. NMDA receptor function and regulation are essential for numerous forms of synaptic plasticity and for spatial learning (reviewed in Bliss and Collingridge, 1993). Complete loss of NMDA and non-NMDA glutamate receptor subunits led to defects in LTP (Zamanillo et al., 1999, and references within). Deletion of PSD-95, an important structural component of the NMDA receptor complex (Migaud et al., 1998) did not lead to defects in NMDA receptor subunit expression, but rather shifted the frequency function of NMDA-dependent LTP and LTD to greatly enhanced LTP. Our data show that, at CA3-CA1 synapses, loss of EphB2 has little or no effects on the induction and maintenance of early phase LTP, which, according to present models, has a strong postsynaptic component (reviewed in Soderling and Derkach, 2000). Long-lasting LTP, which is thought to involve structural remodeling at pre- and postsynaptic sites was, however, affected in EphB2-deficient mice. One of the roles of EphB2 at adult synapses may be to mediate structural changes during plasticity processes by signaling to the actin cytoskeleton (reviewed in Wilkinson, 2000). This function of ephrin/Eph may be completely independent of the NMDAR and may instead involve other components of the PSD such as PDZ domain containing proteins. Interestingly, chemical inhibition of actin filament assembly was recently shown to block maintenance of LTP, leaving basal synaptic transmission and induction of LTP unaffected, a phenotype strikingly similar to *EphB2*$^{-/-}$ mice (Krucker et al., 2000). EphrinB/EphB signaling to the actin cytoskeleton may therefore positively regulate long lasting LTP.

Our results show that *EphB2*$^{-/-}$ hippocampal slices show markedly reduced LTD in juveniles and depotentiation in adults. LTD could be induced but it was not stabilized in *EphB2*$^{-/-}$ mice compared to controls. Similarly, low frequency stimulation did not reduce potentiation after LTP to baseline levels as observed in controls. Both forms of synaptic depression share common characteristics, such that they are induced by low-frequency stimulation, require NMDA receptor activation and signaling via the cAMP-protein kinase A (PKA) pathway, and are blocked by inhibitors of protein phosphatases (reviewed in Wagner and Alger, 1996). Studies in mutant mice have shown that the Cβ_1 subunit of PKA is required for long-lasting LTP and for LTD and depotentiation in the CA3-CA1 pathway (Qi et al., 1996). The serine/threonine-protein phosphatase calcineurin Aα is specifically required for depotentiation, but not LTD, indicating the presence of specific signaling pathways (Zhuo et al., 1999). So far, there is no direct biochemical link between the ephrinB/EphB signaling system and PKA/calcineurin, and they may represent parallel pathways. Alternatively, PKA and calcineurin may modulate NMDA receptor function, which in turn may have effects on the ephrinB/EphB system.

Kinase-Deficient EphB2 Rescues the *EphB2*$^{-/-}$ Phenotype

Because LTP is a prominent feature in brain regions involved in learning and memory, LTP is considered the best cellular model for long-term memory (Bliss and Collingridge, 1993). Deficits in LTP very often, but not always, correlate with deficits in spatial learning (re-

viewed in Martin et al. 2000; Minichiello et al., 1999; Zamanillo et al., 1999). In our water maze experiment with *EphB2*$^{-/-}$ mice, we find reduced escape performance and a gradual reduction of spatial preference during probe trials. Whether this defect mainly reflects problems in general performance or hippocampal function remains to be established. Interestingly, the noncatalytic EphB2-β-gal fusion protein largely rescued the *EphB2*$^{-/-}$ phenotype, including the lack of interaction with the NR1 subunit of NMDA receptors, the increase in number of CA1 synapses, the lack of depotentiation and reduced L-LTP of the CA3-CA1 pathway, and impaired maze performance (see also Henderson et al., 2001 [this issue of *Neuron*]). These findings demonstrate that EphB2 receptors do not require an active kinase domain to mediate most of its known functions. In previous studies (Henkemeyer et al., 1996; Orioli et al., 1996), we proposed the idea that EphB2-β-gal is signaling deficient and would mediate its functions by interacting with axonal ephrinB ligands, which may themselves act like signaling receptors. We now find that a proportion of EphB2-β-gal carries juxtamembrane phosphotyrosine residues. It remains to be demonstrated whether these residues are capable of docking signaling molecules including Src family kinases (reviewed in Wilkinson, 2000). It is possible that a coexpressed Eph receptor (EphA4 or EphB3), upon interaction with the same ephrinB ligand, or a coexpressed receptor from a distantly related RTK subfamily, can transphosphorylate EphB2-β-gal and endow it with some signaling potential. Heterodimerization and cross-talk between different RTKs have previously been described (Follenzi et al., 2000) and represent attractive possibilities for regulation. However, transphosphorylation of this allele has so far not been reported. Whatever the residual signaling potential may be, EphB2-β-gal is noncatalytic and mediates its functions in a kinase-independent fashion.

We conclude that the interaction of EphB2 with NMDA receptors mediates changes in excitatory synapses, thereby regulating their response to stimuli inducing LTP, LTD, and depotentiation. Some of these changes may require direct EphB2/NR1 association; others may be mediated by indirect cross-talk further downstream in the signaling pathways involving ERKs, CREB, and/or Src family kinases. The rescue with kinase-deficient EphB2 suggests that coclustering per se modulates NMDAR function and argues for a signaling role of postsynaptic ephrinB ligands. Changes in synaptic strength will influence performance in behavioral assays. Exactly which neuronal pathways are modulated by ephrin/Eph signaling is currently not known and will require more specifically targeted genetic tools.

Experimental Procedures

Mice

The generation and genotypic analysis of *EphB2*$^{-/-}$, *EphB2*^{lacZ}, and *EphB3*$^{-/-}$ mutant mice has been described previously (Henkemeyer et al., 1996; Orioli et al., 1996). Mutant mice were maintained in a heterozygous state on a 129xC57Bl/6 background.

Primary Culture

Cortical and hippocampal neuron cultures were prepared from E16.5 CD1 mouse embryos and cultured for 7 DIV in Neuralbasal media plus B27 (GIBCO). For stimulation with clustered EphrinB1 ligand, EphrinB1-Fc (R&D) was incubated in an anti-human antibody (R&D) for 1–2 hr on ice. Clustered ligand (0.5–2 μg/ml) was added directly to the dish, and subsequently cells were harvested at different time points for biochemical assays. For stimulation with glutamate (50 μM), cells were washed twice in HBSS without Mg^{2+} (GIBCO) prior to 5 min incubation with glutamate in HBSS without Mg^{2+}. Following stimulation, cells were harvested for biochemical assays.

Brain Tissue Biochemistry

Brain tissues were homogenized in lysis buffer (50 mM Tris [pH 7.5], 120 mM NaCl, 0.5% Triton X-100, 1 mM sodium orthovanadate) and protease inhibitors (complete tablets, Roche). Samples were incubated with specific antibodies and protein A- or G-conjugated sepharose beads (Amersham) for 1–2 hr at 4°C. Samples were washed three times in lysis buffer and eluted with 2× SDS sample buffer (10% Glycerol, 3% SDS, 3% DTT). Eluates were run on a SDS page. Western blotting was performed according to general procedures. Precipitates and coprecipitates were detected using specific primary antibodies and HRP-conjugated secondary antibodies (Amersham) and visualized using ECL. Antibodies: anti-(SAM)EphB2, rabbit polyclonal antiserum raised against the SAM domain of mouse EphB2 fused to GST (1:3000), anti-phospho-EphB2 (Dalva et al., 2000) (1:1500), anti-β-galactosidase (Cappel, 1:1000), and anti NR1-antibody (Pharmingen, 1:1500).

Biochemical Assays

Cortical and hippocampal neurons at 7DIV were lysed in Lysis buffer (50 mM Tris [pH 7.5.], 120 mM NaCl, 1% Triton X-100, 1 mM sodium orthovanadate, 10 mM NaF, 1 mM NaPP, and 10 mM β-glycerophosphate) and protein inhibitors (complete tablets, Roche). For the phospho-MAPK assay, 60 μg total protein was loaded on a 15% Anderson gel and analyzed via Western blotting with a phospho-MAPK antibody (Biolabs, 1:2000). For CREB activation, 60 μg total protein was loaded on 12% SDS-page, blotted with anti-phospho-CREB antibody (Upstate biotechnology, 1:1000) Autophosphorylation of EphB2 receptor was monitored by immunoprecipitation with the anti-(SAM)EphB2 antibody, and Western blotting with anti-phosphotyrosine-antibody (Upstate biotechnology, 1:1500). EphB2 protein levels were assayed with immunoprecipitation and Western blotting with the anti-(SAM)EphB2 antibody.

Immunostaining

Cells were stimulated for 60 min with clustered, activated ephrinB1-Fc (2 μg/μl) and fixed for 10 min with 4% paraformaldehyde in PBS. Neurons were stained with anti-NR1 (Pharmingen) for 2–3 hr at room temperature. Secondary anti-mouse conjugated with Texas red (1:200) to detect NR1 sites, and secondary anti-Goat-Alexa488 (1:200) to detect preclustered ephrinB1-Fc were applied for 1 hr at room temperature. Nuclei were stained with Hoechst before mounting.

Imaging and Image Analysis

Confocal images were acquired using constant settings on a Leica TCS NT inverted microscope with a 63× oil objective using the Leica TCS software. Cells for analysis were selected with the experimenter blind in respect to genotype. Using NIHImage software, NR1 and EphB sites in a defined area were counted that met size criteria (~0.09 μm^2). Coclusters were analyzed using a special macro for NIHImage. Statistical analysis was done using StatView software.

Histology, In Situ Hybridization Analysis, and Electron Microscopy

Histological and immunochemical analyses were carried out as described (Minichiello et al., 1999). Synapse counts were done with the experimenter blind regarding the genotype of the mice. Synapses were counted on photographs at a magnification of 5510× on 70–110 pictures, ca. 3000–5000 synapses per genotype. The data was analyzed using Statview Anova software. Mice were perfused with 4% paraformaldehyde. 100 μm vibratome sections were processed according to standard procedures for in situ hybridization. Probes were detected with an alkaline phosphatase-conjugated anti-digoxygenin antibody (Roche, 1:2000) and BM purple substrate (Roche).

Behavioral Tests

The Morris navigation test was carried out in an open-field water maze of 1.5 m in diameter and filled with opaque water at the temperature of 25°C ± 1°C, located in a laboratory that contained prominent extra maze cues. A hidden 15 cm diameter platform was used. Trials lasted a maximum of 120 s. Spatial training consisted of 18 trials (six per day, separated by an interval of about 30 min), during which the platform was left in the same position. After 3 days of learning, the platform was moved to the opposite position, and reversal learning was monitored for 2 additional days (six trials per day).

Electrophysiological Recordings

The *EphB2*$^{-/-}$ and *EphB2*$^{lacZ/lacZ}$ mice were between P40 and P73 for depotentiation and LTP (E-LTP, L-LTP) experiments; for LTD experiments, mice were between P14 and P20. The ACSF was saturated with 95% O_2/5% CO_2 and contained (in mM): NaCl, 124.0; KCl, 3.0; KH_2PO_4, 1.25; $NaHCO_3$, 26.0; $MgSO_4$, 2.0; $CaCl_2$, 2.5; Glucose, 10.0. The hippocampi were cut into 400 μm-thick transversal. Slices were maintained in ACSF at room temperature for at least 1.5 hr before recording. Recordings were started after a 20 min equilibration phase in the recording chamber. Synaptic responses were evoked in the CA3 region of the mouse hippocampus by stimulating Schaffer collaterals with 0.1 ms pulse duration through monopolar tungsten electrodes. Field excitatory postsynaptic potentials (fEPSPs) were recorded extracellularly in the *stratum radiatum* of the CA1 pyramidal cell region (~100 μm below slice surface) using glass microelectrodes (borosilicate: 1.0 mm OD × 0.58 mm ID + inner filament; Clark, Reading, England) filled with 3 M NaCl (8–20 MOhm). For baseline recordings, the slices were stimulated at 0.1 Hz for 20 min at stimulation intensities that resulted in half-maximal fEPSP amplitudes (30–180 mA). Paired-pulse facilitation (PPF) was tested by applying two pulses separated by intervals ranging from 10–160 ms. To induce LTD, a 1 Hz stimulus train was delivered for 15 min (900 pulses) with the same intensity used for recording the baseline. For depotentiation experiments, 10 min after a theta-burst stimulation (100 Hz, 3× TBS), a 1 Hz stimulus train of 5 min (300 pulses) or 15 min (900 pulses) duration was given. LTP was induced by applying theta-burst stimulation (TBS). TBS consists of three bursts (10 s interval), each of them composed of ten trains (5 Hz) with four pulses each (100 Hz). To analyze the functionality of the NMDA receptor, extracellular field EPSPs were recorded in the following sequence: 15 min of baseline recording with normal ACSF, 15 min application of 10 μM DNQX (in ACSF with low Mg^{2+} [0.5 mM] and high Ca^{2+} [4 mM]); 10 min of 50 μM AP-5 application in addition to the DNQX medium (again low Mg^{2+} and high Ca^{2+}), 1 hr washout time.

Data Analysis

Electrophysiological data were sampled at 5 kHz on a PC using a customized LabView program (National Instruments, Austin, TX), which was also used for offline analysis. All measurements were carried out and analyzed in a strictly blind fashion. Therefore, the genotype of an experiment was only analyzed and revealed after the measurement and its analysis had been completed. As an indicator of synaptic strength, the initial slope of the evoked fEPSPs was calculated, averaged across six consecutive measurements and expressed as percentages relative to the baseline mean. The normalized data of each experiment were then time-matched, averaged across experiments, and expressed as means (±SEM). PPF was expressed as the increase in initial slope of the second fEPSP relative to the first. Posttetanic potentiation (PTP) was measured as the mean fEPSP slope during the first 3 min after the application of TBS relative to baseline.

Acknowledgments

We thank B. Brühl, V. Staiger, R. Mandani, R. Lang, and I. Drescher for expert help; M. Greenberg, M.B. Dalva, and associates for sharing results before publication and for reagents; J. Rietdorf for expert help with analysis of confocal images; and K. Kullander for comments on the manuscript. This study was in part supported by grants from the Deutsche Forschungsgemeinschaft (DFG) and the Human Frontier Science Programme Organization (HFSPO), the EC Biotech Programme (BIO4CT980297/BBW98.0125), the Max-Planck Society, the NCCR on Neural Plasticity and Repair, and the Swiss National Science Foundation (SNF 31-57139.99 and 31-54184.98).

Received February 26, 2001; revised October 18, 2001.

References

Adams, R.H., Wilkinson, G.A., Weiss, C., Diella, F., Gale, N.W., Deutsch, U., Risau, W., and Klein, R. (1999). Roles of ephrinB ligands and EphB receptors in cardiovascular development: demarcation of arterial/venous domains, vascular morphogenesis and sprouting angiogenesis. Genes Dev. *13*, 295–306.

Ali, D.W., and Salter, M.W. (2001). NMDA receptor regulation by Src kinase signalling in excitatory synaptic transmission and plasticity. Curr. Opin. Neurobiol. *11*, 336–342.

Birgbauer, E., Cowan, C.A., Sretavan, D.W., and Henkemeyer, M. (2000). Kinase independent function of EphB receptors in retinal axon pathfinding to the optic disc from dorsal but not ventral retina. Development *127*, 1231–1241.

Bjorge, J.D., Jakymiw, A., and Fujita, D.J. (2000). Selected glimpses into the activation and function of src kinase. Oncogene *19*, 5620–5635.

Bliss, T.V.P., and Collingridge, G.L. (1993). A synaptic model of memory: long-term potentiation in the hippocampus. Nature *361*, 31–39.

Bourtchuladze, R., Frenguelli, B., Blendy, J., Cioffi, D., Schutz, G., and Silva, A.J. (1994). Deficient long-term memory in mice with a targeted mutation of the cAMP-responsive element-binding protein. Cell *79*, 59–68.

Brückner, K., and Klein, R. (1998). Signalling by Eph receptors and their ephrin ligands. Curr. Opin. Neurobiol. *8*, 375–382.

Buchert, M., Schneider, S., Meskenaite, V., Adams, M.T., Canaani, E., Baechi, T., Moelling, K., and Hovens, C.M. (1999). The junction-associated protein AF-6 interacts and clusters with specific Eph receptor tyrosine kinases at specialized sites of cell-cell contact in the brain. J. Cell Biol. *144*, 361–371.

Cowan, C.A., Yokoyama, N., Bianchi, L.M., Henkemeyer, M., and Fritzsch, B. (2000). EphB2 guides axons at the midline and is necessary for normal vestibular function. Neuron *26*, 417–430.

Dalva, M.B., Takasu, M.A., Lin, M.Z., Shamah, S.M., Hu, L., Gale, N.W., and Greenberg, M.E. (2000). EphB receptors interact with NMDA receptors and regulate excitatory synapse formation. Cell *103*, 945–956.

Drescher, U. (2000). Excitation at the synapse: Eph receptors team up with NMDA receptors. Cell *103*, 1005–1008.

Dudek, S.M., and Bear, M.F. (1993). Bidirectional long-term modification of synaptic effectiveness in the adult and immature hippocampus. J. Neurosci. *13*, 2910–2918.

Flanagan, J.G., and Vanderhaeghen, P. (1998). The ephrins and Eph receptors in neural development. Annu. Rev. Neurosci. *21*, 309–345.

Follenzi, A., Bakovic, S., Gual, P., Stella, M.C., Longati, P., and Comoglio, P.M. (2000). Cross-talk between the proto-oncogenes Met and Ron. Oncogene *19*, 3041–3049.

Gallagher, M., Burwell, R., and Burchinal, M. (1993). Severity of spatial learning impairment in aging: development of a learning index of performance in the Morris water maze. Behav. Neurosci. *107*, 618–626.

Gao, W.Q., Shinsky, N., Armanini, M.P., Moran, P., Zheng, J.L., Mendoza-Ramirez, J.L., Phillips, H.S., Winslow, J.W., and Caras, I.W. (1998). Regulation of hippocampal synaptic plasticity by the tyrosine kinase receptor, REK7/EphA5, and its ligand, AL-1/Ephrin-A5. Mol. Cell. Neurosci. *11*, 247–259.

Garner, C.C., Nash, J., and Huganir, R.L. (2000). PDZ domains in synapse assembly and signalling. Trends Cell Biol. *10*, 274–280.

Gerlai, R., Shinsky, N., Shih, A., Williams, P., Winer, J., Armanini, M., Cairns, B., Winslow, J., Gao, W., and Phillips, H.S. (1999). Regulation of learning by EphA receptors: a protein targeting study. J. Neurosci. *19*, 9538–9549.

Grant, S.G., O'Dell, T.J., Karl, K.A., Stein, P.L., Soriano, P., and Kandel, E.R. (1992). Impaired long-term potentiation, spatial learning, and hippocampal development in fyn mutant mice. Science *258*, 1903–1910.

Henderson, J.T., Georgiou, J., Jia, Z., Robertson, J., Elowe, S., Roder, J.C., and Pawson, T. (2001). The receptor tyrosine kinase EphB2 regulates NMDA-dependent synaptic function. Neuron *32*, this issue, 1041–1056.

Henkemeyer, M., Orioli, D., Henderson, J.T., Saxton, T.M., Roder, J., Pawson, T., and Klein, R. (1996). Nuk controls pathfinding of commissural axons in the mammalian central nervous system. Cell *86*, 35–46.

Husi, H., Ward, M.A., Choudhary, J.S., Blackstock, W.P., and Grant, S.G. (2000). Proteomic analysis of NMDA receptor-adhesion protein signaling complexes. Nat. Neurosci. *3*, 661–669.

Impey, S., Obrietan, K., Wong, S.T., Poser, S., Yano, S., Wayman, G., Deloulme, J.C., Chan, G., and Storm, D.R. (1998). Cross talk between ERK and PKA is required for Ca2+ stimulation of CREB-dependent transcription and ERK nuclear translocation. Neuron *21*, 869–883.

Impey, S., Obrietan, K., and Storm, D.R. (1999). Making new connections: role of ERK/MAP kinase signaling in neuronal plasticity. Neuron *23*, 11–14.

Kang, H., Sun, D.L., Atkins, C.M., Soderling, T.R., Wilson, M.A., and Tonegawa, S. (2001). An Important role of neural activity-dependent CaMKIV signaling in the consolidation of long-term memory. Cell *106*, 771–783.

Kano, M., Hashimoto, K., Chen, C., Abeliovich, A., Aiba, A., Kurihara, H., Watanabe, M., Inoue, Y., and Tonegawa, S. (1995). Impaired synapse elimination during cerebellar development in PKC gamma mutant mice. Cell *83*, 1223–1231.

Katz, L.C., and Shatz, C.J. (1996). Synaptic activity and the construction of cortical circuits. Science *274*, 1133–1138.

Kavalali, E.T., Klingauf, J., and Tsien, R.W. (1999). Activity-dependent regulation of synaptic clustering in a hippocampal culture system. Proc. Natl. Acad. Sci. USA *96*, 12893–12900.

Kawasaki, H., Fujii, H., Gotoh, Y., Morooka, T., Shimohama, S., Nishida, E., and Hirano, T. (1999). Requirement for mitogen-activated protein kinase in cerebellar long term depression. J. Biol. Chem. *274*, 13498–13502.

Klein, R. (2001). Excitatory Eph receptors and adhesive ephrin ligands. Curr. Opin. Cell Biol. *13*, 196–203.

Krucker, T., Siggins, G.R., and Halpain, S. (2000). Dynamic actin filaments are required for stable long-term potentiation (LTP) in area CA1 of the hippocampus. Proc. Natl. Acad. Sci. USA *97*, 6856–6861.

Martin, S.J., Grimwood, P.D., and Morris, R.G. (2000). Synaptic plasticity and memory: an evaluation of the hypothesis. Annu. Rev. Neurosci. *23*, 649–711.

Meyer, B.U., Roricht, S., and Niehaus, L. (1998). Morphology of acallosal brains as assessed by MRI in six patients leading a normal daily life. J. Neurol. *245*, 106–110.

Miao, H., Wei, B.R., Peehl, D.M., Li, Q., Alexandrou, T., Schelling, J.R., Rhim, J.S., Sedor, J.R., Burnett, E., and Wang, B. (2001). Activation of EphA receptor tyrosine kinase inhibits the Ras/MAPK pathway. Nat. Cell Biol. *3*, 527–530.

Migaud, M., Charlesworth, P., Dempster, M., Webster, L.C., Watabe, A.M., Makhinson, M., He, Y., Ramsay, M.F., Morris, R.G., Morrison, J.H., et al. (1998). Enhanced long-term potentiation and impaired learning in mice with mutant postsynaptic density-95 protein. Nature *396*, 433–439.

Minichiello, L., Korte, M., Wolfer, D., Kühn, R., Unsicker, K., Cestari, V., Rossi-Arnaud, C., Lipp, H.-P., Bonhoeffer, T., and Klein, R. (1999). Essential role for TrkB receptors in hippocampus-mediated learning. Neuron *24*, 401–414.

Morris, R.G.M. (1982). Place navigation impaired in rats with hippocampal lesions. Nature *297*, 681–683.

O'Dell, T.J., and Kandel, E.R. (1994). Low-frequency stimulation erases LTP through an NMDA receptor-mediated activation of protein phosphatases. Learn. Mem. *1*, 129–139.

Orioli, D., Henkemeyer, M., Lemke, G., Klein, R., and Pawson, T. (1996). Sek4 and Nuk receptors cooperate in guidance of commissural axons and in palate formation. EMBO J. *15*, 6035–6049.

Qi, M., Zhuo, M., Skalhegg, B.S., Brandon, E.P., Kandel, E.R., McKnight, G.S., and Idzerda, R.L. (1996). Impaired hippocampal plasticity in mice lacking the Cbeta1 catalytic subunit of cAMP-dependent protein kinase. Proc. Natl. Acad. Sci. USA *93*, 1571–1576.

Shin, D., Garcia-Cardena, G., Hayashi, S.I., Gerety, S., Asahara, T., Stavrakis, G., Isner, J., Folkman, J., Gimbrone, M.A., and Anderson, D.J. (2001). Expression of EphrinB2 identifies a stable genetic difference between arterial and venous vascular smooth muscle as well as endothelial cells, and marks subsets of microvessels at sites of adult neovascularization. Dev. Biol. *230*, 139–150.

Soderling, T.R., and Derkach, V.A. (2000). Postsynaptic protein phosphorylation and LTP. Trends Neurosci. *23*, 75–80.

Takasu, M.A., Dalva, M.B., Zigmond, R.E., and Greenberg, M.E. (2002). Modulation of NMDA Receptor-dependent Calcium influx and gene expression through EphB receptors. Science, in press.

Torres, R., Firestein, B.L., Dong, H., Staudinger, J., Olson, E.N., Huganir, R.L., Bredt, D.S., Gale, N.W., and Yancopoulos, G.D. (1998). PDZ proteins bind, cluster and synaptically co-localize with Eph receptors and their ephrin ligands. Neuron *21*, 1453–1463.

Wagner, J.J., and Alger, B.E. (1996). Homosynaptic LTD and depotentiation: do they differ in name only? Hippocampus *6*, 24–29.

Wilkinson, D.G. (2000). Topographic mapping: organising by repulsion and competition? Curr. Biol. *10*, R447–R451.

Yu, X.M., and Salter, M.W. (1999). Src, a molecular switch governing gain control of synaptic transmission mediated by N-methyl-D-aspartate receptors. Proc. Natl. Acad. Sci. USA *96*, 7697–7704.

Zamanillo, D., Sprengel, R., Hvalby, O., Jensen, V., Burnashev, N., Rozov, A., Kaiser, K., Koster, H., Borchardt, T., Worley, P., et al. (1999). Importance of AMPA receptors for hippocampal synaptic plasticity but not for spatial learning. Science *284*, 1805–1811.

Zhuo, M., Zhang, W., Son, H., Mansuy, I., Sobel, R.A., Seidman, J., and Kandel, E.R. (1999). A selective role of calcineurin alpha in synaptic depotentiation in hippocampus. Proc. Natl. Acad. Sci. USA *96*, 4650–4655.